

## SIMULATIONS OF A FULLY PULSED ROUND TURBULENT AIR JET FLOW WITH $k$ - $\epsilon$ AND REYNOLDS STRESS TURBULENCE MODELS

Magnus NORDSVEEN\* and Klaus BREMHORST

Department of Mechanical Engineering, The University of Queensland  
 Brisbane, Queensland, 4072, AUSTRALIA

### ABSTRACT

Flow of a fully pulsed turbulent round air jet into quiescent air has been simulated applying both the  $k$ - $\epsilon$  and the Reynolds stress turbulence models. Previously published work has shown that the  $k$ - $\epsilon$  model fails to predict the change in slope of the velocity decay where the jet changes from pulsed to steady jet behavior. In the present work it is seen that this deficiency also applies to the Reynolds stress model. However, the Reynolds stress model considerably improves the predictions in the pulsed region. It predicts correctly the magnitude and phase of the sharp velocity transients which is not the case with the  $k$ - $\epsilon$  model.

### INTRODUCTION

Fully pulsed round air jets flowing out of a nozzle in short pulses into stagnant surroundings are considered where fully pulsed means that the exit velocity reduces to zero during the cycle. Bremhorst and Harch (1979), Hollis (1988) and Gehrke (1997) conducted experiments with fully pulsed air jets and reported a significant increase in entrainment over steady jets of the same average nozzle mass flow rates. Consequently, such jets are of interest for mixing operations where the length of the mixing zone is limited. Another characteristic of jets is the centre line axial velocity decay, the inverse of which is linear after an initial development length. Bremhorst and Harch (1979) showed that for a fully pulsed jet the time averaged centre line axial velocity decay was much slower than for a steady jet. However, Hollis (1988) and Gehrke (1997) reported that after about 50 diameters downstream of the nozzle exit, the time averaged centre line axial velocity decay for a fully pulsed jet changes to the steady jet rate.

Graham and Bremhorst(1993) used a  $k$ - $\epsilon$  model to simulate a fully pulsed air jet. They found that the model predicted the velocity decay for the pulse dominated region of the jet well, but failed to predict the change in slope further downstream unless one of the constants in the model was changed at the position where the jet becomes less pulse dominated. The need for this change arose from the observation that predicted turbulent kinetic energy decayed far too rapidly with downstream distance. An increase in  $c_{2\epsilon}$  led to a recovery of turbulent kinetic energy to a level comparable with the measured one. Furthermore, Gehrke (1997) found in his measurements for fully pulsed round free jets, the existence of negative production of turbulent kinetic energy. This effect cannot

be modelled with the  $k$ - $\epsilon$  model and motivated the present work where fully pulsed air jets are simulated with both the Reynolds stress model and the  $k$ - $\epsilon$  model with a closer examination of the turbulent kinetic energy balance.

### MATHEMATICAL MODELS

The flow is assumed incompressible and Newtonian and the computations are based on the phase-averaged (denoted by an overbar for turbulence cross-products) axisymmetric continuity and Navier-Stokes equations. Applying tensor notation and the Einstein summation convention the continuity equation becomes  $\partial U_i / \partial x_i = 0$ . The Reynolds averaged momentum equations are:

$$\frac{\partial \rho U_i}{\partial t} + \frac{\partial \rho U_i U_j}{\partial x_j} = -\frac{\partial P}{\partial x_i} + \frac{\partial}{\partial x_j} \left( \mu \frac{\partial U_i}{\partial x_j} - \overline{\rho u_i u_j} \right).$$

#### The $k$ - $\epsilon$ Turbulence Model

When using the  $k$ - $\epsilon$  turbulence model the Reynolds stresses are described with the generalized Boussinesq hypothesis:

$$-\overline{\rho u_i u_j} = R_{ij} = \nu_t \left( \frac{\partial U_i}{\partial x_j} + \frac{\partial U_j}{\partial x_i} \right) - \frac{2}{3} \rho k \delta_{ij}$$

where the eddy viscosity is given by  $\nu_t = c_\mu \frac{k^2}{\epsilon}$ . The turbulent kinetic energy,  $k$ , and its dissipation rate,  $\epsilon$ , are represented by the following transport equations (Rodi, 1980):

$$\frac{\partial \rho k}{\partial t} + \frac{\partial U_i \rho k}{\partial x_i} = \frac{\partial}{\partial x_i} \left( \frac{\mu_t}{\sigma_k} \frac{\partial k}{\partial x_i} \right) + R_{ij} \frac{\partial U_i}{\partial x_j} - \rho \epsilon,$$

$$\frac{\partial \rho \epsilon}{\partial t} + \frac{\partial U_i \rho \epsilon}{\partial x_i} = \frac{\partial}{\partial x_i} \left( \frac{\mu_t}{\sigma_\epsilon} \frac{\partial \epsilon}{\partial x_i} \right) + \left( c_{1\epsilon} R_{ij} \frac{\partial U_i}{\partial x_j} - c_{2\epsilon} \rho \epsilon \right) \frac{\epsilon}{k}$$

\*Present affiliation: Studsvik Scandpower AS, P.O. Box 15, 2007 Kjeller, Norway

The constants applied in the k-ε model are given in Table 1.

$c_\mu$	$\sigma_k$	$\sigma_\varepsilon$	$c_{1\varepsilon}$	$c_{2\varepsilon}$
0.09	1.0	1.3	1.44	1.92

**Table 1:** Constants in the k-ε model (Launder et al, 1975, Rodi, 1980)

### The Reynolds Stress Model

In the Reynolds stress model, (rst), transport equations for the Reynolds stresses are solved. The turbulent kinetic energy is calculated as half the sum of the normal stresses and the dissipation rate is governed by another transport equation. The equations used for the Reynolds stresses are essentially the ones proposed by Launder et al (Rodi, 1980 and Launder, 1975) where the isotropization-of-production model has been used for the pressure strain term and a simplified form of the Daly-Harlow model has been used for diffusion. The Reynolds stress equations read:

$$\frac{\partial \overline{\rho u_i u_j}}{\partial t} + \frac{\partial U_k \overline{\rho u_i u_j}}{\partial x_k} = \frac{\partial}{\partial x_k} \left( \overline{c_s u_k u_k} \frac{k}{\varepsilon} \frac{\partial \overline{\rho u_i u_j}}{\partial x_k} \right) + P_{ij} + \phi_{ij} - \rho \varepsilon \delta_{ij}$$

where the stress production is given by:

$$P_{ij} = -\rho \left( \overline{u_k u_i} \frac{\partial U_j}{\partial x_k} + \overline{u_k u_j} \frac{\partial U_i}{\partial x_k} \right)$$

The pressure strain term  $\phi_{ij}$  is modelled as:

$$\phi_{ij} = -c_1 \overline{\rho u_i u_j} - \frac{2}{3} \delta_{ij} \overline{\rho k} \frac{\varepsilon}{k} - c_2 (P_{ij} - \frac{1}{3} \delta_{ij} P_{kk})$$

and the dissipation rate is given by the equation:

$$\frac{\partial \rho \varepsilon}{\partial t} + \frac{\partial U_i \rho \varepsilon}{\partial x_i} = \frac{\partial}{\partial x_i} \left( \overline{c_\varepsilon u_i u_i} \frac{k}{\varepsilon} \frac{\partial \rho \varepsilon}{\partial x_i} \right) + \left( c_{1\varepsilon} \frac{P_{kk}}{2} - c_{2\varepsilon} \rho \varepsilon \right) \frac{\varepsilon}{k}$$

The values of the constants in the Reynolds stress model are listed in Table 2.

$c_\varepsilon$	$c_{1\varepsilon}$	$c_{2\varepsilon}$	$c_s$	$c_1$	$c_2$
0.18	1.45	1.90	0.22	1.8	0.6

**Table 2:** Constants in the Reynolds stress model (Launder et al, 1975 and Cham Ltd)

### Boundary and initial conditions

The calculation domain extends from the exit of the nozzle to 120 nozzle diameters downstream in the axial direction with a radial width of 50 nozzle diameters. First the steady state jet was solved for an axial velocity out of the nozzle of 36.6 m/s which is equal to that used in the experimental work. The pulsed jet simulation was started from the steady jet flow prediction. For the pulsed jet, the time dependent non-zero axial velocity was based on the data of Hollis (1988) at one diameter downstream of the nozzle exit and modelled as:

$$U_{\text{exit}}(\tau) = 2U_{\text{exit}} \frac{\tau_c}{\tau_e} \sin^2\left(\frac{\tau\pi}{\tau_e}\right), \quad 0 < \tau < \tau_e,$$

where  $U_{\text{exit}} = 36.6$  m/s, the cycle time,  $\tau_c$ , equals to 0.1 second, the pulse duration,  $\tau_e$ , equals 0.0333 second and  $\tau$  is the time through the pulse. The nozzle is closed with zero outflow for 2/3 of the cycle. The inlet conditions for other quantities are given in Table 3. Radial velocity and shear stress are set equal to zero at the inlet.

	$k_{in}$	$\varepsilon_{in}$	$\overline{u_i u_i}$
Steady jet	$0.01 * U_{\text{exit}}^2$	$0.1643 * (k_{in}^{1.5} / (0.035d))$	$2/3 * k_{in}$
Pulsed jet	$0.04 * U^2(\tau)$	$0.1643 * (k_{in}^{1.5} / (0.035d))$	$2/3 * k_{in}$

**Table 3:** Inlet boundary conditions (d = nozzle diameter)

The outer part of the inlet plane, extending from the nozzle edge to the free stream plane, was modelled as a frictionless wall. A fixed pressure condition was used at the free stream plane with zero gradient conditions for the other variables. At the downstream plane a zero gradient condition was applied to the axial velocity. Symmetry conditions were applied at the axis for all variables except  $V$  and  $\overline{uv}$  which were set to zero. The initial conditions for the steady k-ε simulations were top hat profiles for  $U$ ,  $k$  and  $\varepsilon$  with  $V$  and  $P$  equal to zero. The initial conditions for the steady Reynolds stress calculations were flow fields based on the k-ε simulations.

### THE NUMERICAL METHOD

The CFD code PHOENICS was used to solve the models outlined above. A control volume method with a staggered grid and a backward-Euler implicit time integration scheme was applied. The equation solver is elliptic and the equations for the dependent variables are solved sequentially using the SIMPLE algorithm. The time step was controlled by a Courant-Friedrichs-Lewy criterion (based on the fluid velocity) as well as a maximum change in the nozzle exit velocity of 1 m/s. The simulations were performed with 108 and 206 control volumes in the radial and axial directions, respectively.



## RESULTS

Two simulations corresponding to Hollis' (1988) and Gehrke's (1997) experimental cases were performed. The difference between the two is that Hollis used a nozzle with 25.4 mm diameter while Gehrke's nozzle diameter was 12.7 mm. Gehrke did not measure the flow field close to the nozzle exit and we have used Hollis' data for both cases. In Figure 1 the averaged axial velocity along the centre line for Hollis' case is presented.  $x$  denotes axial distance and  $d$  denotes nozzle diameter. It is seen that the  $k-\epsilon$  and the Reynolds stress models agree well with the experimental results up to about 50 diameters. However, the change in slope is not captured correctly with the models. It is also seen that after 50 diameters the slope for Hollis' pulsed jet experiments is very similar to the slope for Panchapakesan and Lumley's (1993) experimental results for a steady jet. In the simulations the startup vortex generated by the pulse travels downstream with the pulse and disintegrates about 50 diameters from the nozzle exit where pulse domination is seen to become negligible.

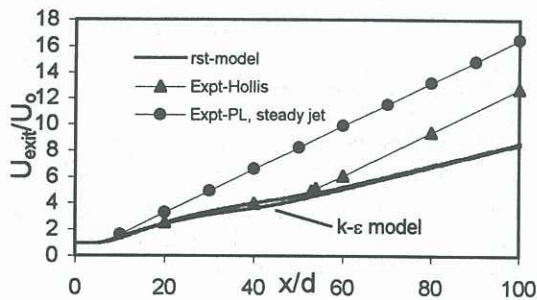


Figure 1: Decay of mean axial velocity.

In Figure 2 through pulse jet centre line axial velocity at  $x/d = 1, 20$  and  $40$  for Hollis' case is presented. It is seen that both the phase and the amplitude of the velocity transient are predicted very well with the Reynolds stress model while the predictions with the  $k-\epsilon$  model become increasingly incorrect with distance from the nozzle exit. At  $x/d = 60$ , which is used for subsequent discussions, the pulse is still clearly visible when viewing phase averaged velocities through the pulse, but its r.m.s. value is comparable to that of the intrinsic velocity fluctuations (Hollis, 1988).

Although not shown here, pulse averaged turbulent kinetic energies at the centre line for the rst model decayed very rapidly in the streamwise direction just as found by Graham and Bremhorst (1993) with the  $k-\epsilon$  model. This may almost be expected as the rst model has a similar destruction term in the  $\epsilon$  transport equation to that of the  $k-\epsilon$  model.

Figure 3 (predictions) and Figure 4 (measurements) give the averaged radial profiles at  $x/d=60$  of the different terms in the turbulent kinetic energy balance for Gehrke's case.  $r$  and  $r_{1/2}$  denote radial distance and jet half width, respectively. It is observed that the measured production term diminishes to zero towards the axis. This is not

captured in the simulation. The explanation for this may be found in Figure 5 (predictions, where  $PK1 \approx PK2$ ) and Figure 6 (experiments) where the various through pulse turbulent kinetic energy production terms at the axis at  $x/d=60$  are shown ( $PK1 = \overline{\rho v^2 dV/dr}$ ,  $PK2 = \overline{\rho w^2 V/r}$ ,  $PK3 = \overline{\rho u^2 dU/dx}$ ,  $PK4 = \overline{\rho uv(dV/dx + dU/dr)}$ ).

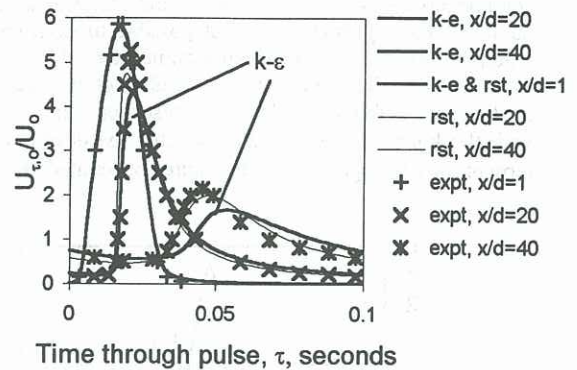


Figure 2: Through pulse jet centre line mean axial velocity at  $x/d = 1, 20$  and  $40$ , Hollis' case.

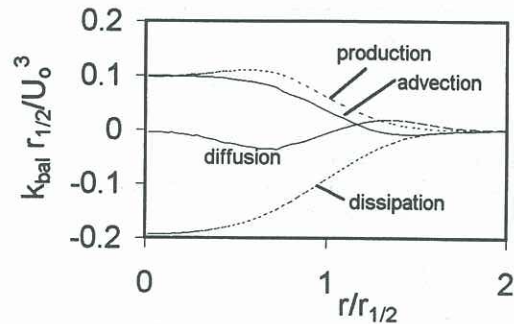


Figure 3: Pulse averaged turbulent kinetic energy balance with the rst model at  $x/d = 60$  for Gehrke's case.

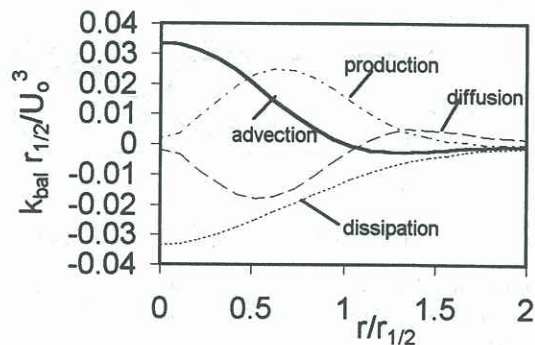


Figure 4: Pulse averaged turbulent kinetic energy balance, radial profiles at  $x/d = 60$ , experimental data of Gehrke.

It is seen that the PK3 term containing the axial mean velocity gradient dominates and the predicted one has a negative section during the later stages of the pulse as found by experiment. However, the PK1 and PK2 components are less pronounced. Combined with the smaller negative value of PK3, the net result is a larger turbulent kinetic energy production than obtained by measurement. A significant difference also exists between magnitudes of measured and predicted components of production. Due to the highly coupled nature of the equations, it is not possible to determine readily which constant or which term needs modification to rectify this deficiency until a number of parametric studies are performed. However, based on experience with the k-ε model, indications are that the destruction term of the ε transport equation requires better modelling.

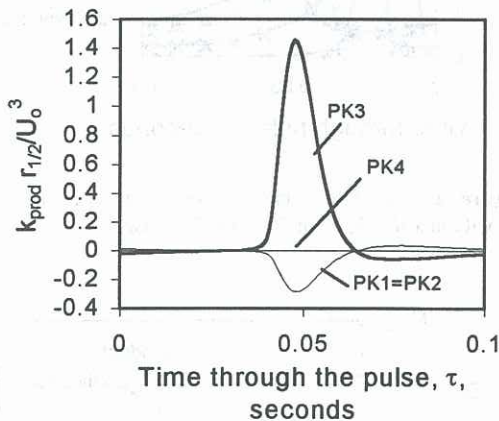


Figure 5: Through pulse turbulent kinetic energy production  $3/16d$  from the axis at  $x/d=60$  for the Reynolds stress model, Gehrke's case.

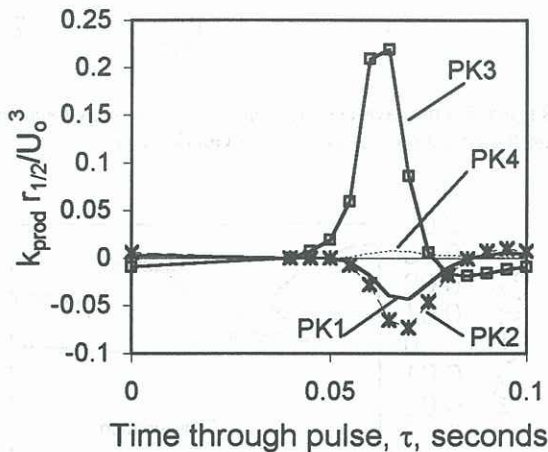


Figure 6: Through pulse turbulent kinetic energy production at the axis at  $x/d=60$ , experimental data of Gehrke.

## CONCLUSION

The fully pulsed turbulent round air jet issuing into quiescent air has been simulated applying both the k-ε and the Reynolds stress turbulence models. The Reynolds

stress model correctly predicted the amplitude and phase of the sharp velocity transients which were smoothed out by the k-ε model. However, both models failed to predict the change in slope of the velocity decay where the jet changed from pulse to steady jet behavior.

An examination of the turbulent kinetic energy balance shows significant differences both in magnitude of the individual components of the k transport equation as well as in the behaviour of the production term as the jet centre line is approached. A preliminary view is that better modelling of the destruction term in the ε transport equation is needed.

## REFERENCES

- BREMHORST, K. and HARCH, W. H. (1979), "Near field velocity measurements in a fully pulsed subsonic air jet", *Turbulent Shear Flows I*, ed, Durst F., Launder B. E., Schmidt F. W. and Whitelaw J. H., Springer Verlag, Berlin, pp. 37.
- DALEY, B. J. and HARLOW, F. H. (1970). "Transport equations of turbulence", *Phys. Fluids*, **13**, pp 2634.
- GEHRKE P. J. (1997), "The turbulent kinetic energy balance of a fully pulsed axisymmetric jet". *Ph.D.Thesis*, The University of Queensland, Brisbane, Australia. Also, with BREMHORST, K., 11th Symposium on Turbulent Shear Flows, Institut. National Polytechnique, Universite Joseph Fourier, Grenoble, 22.1 - 22.6, Sept. 8-10, 1997
- GRAHAM, L. J. W. and BREMHORST, K. (1993) "Application of the k-ε turbulence model to the simulation of a fully pulsed free air jet", *Transactions of the ASME*, **115**, pp. 70.
- HOLLIS, P. G. (1988), "Velocity field investigation of a fully pulsed air jet with a laser Doppler anemometer", *Ph.D. Thesis*, The University of Queensland, Brisbane, Australia. Also, with BREMHORST, K., *AIAA J.*, **28**, 12, 2043-2049, 1990.
- LAUNDER, B. E., REECE, G. J. and RODI, W. (1975). "Progress in the development of a Reynolds stress turbulence closure", *JFM*, **68**, pp 537.
- LAUNDER, B. E. (1975). "On the effect of a gravitational field on the turbulence transport of heat and momentum", *JFM*, **67**, pp. 569.
- PANCHAPAKESAN, N. R. and LUMLEY, J. L. (1993). "Turbulence measurements in axisymmetric jets of air and helium. Part 1. Air jet", *JFM*, **246**, pp. 197.
- RODI, W. (1980), "Turbulence models and their application in hydraulics". *IAHR Book Publication*, Delft, Netherlands.